Neurological Sciences (2021) 42:5289–5296
https://doi.org/10.1007/s10072-021-05255-6

ORIGINAL ARTICLE

A nomogram to predict rupture risk of middle cerebral artery aneurysm

Jinjin Liu[1] · Yongchun Chen[1] · Dongqin Zhu[1] · Qiong Li[1] · Zhonggang Chen[1] · Jiafeng Zhou[1] · Boli Lin[1] · Yunjun Yang[1] · Xiufen Jia[1]

Received: 20 January 2021 / Accepted: 10 April 2021 / Published online: 15 April 2021

Abstract

Background Determining the rupture risk of unruptured intracranial aneurysm is crucial for treatment strategy. The purpose of this study was to predict the rupture risk of middle cerebral artery (MCA) aneurysms using a machine learning technique.

Methods We retrospectively reviewed 403 MCA aneurysms and randomly partitioned them into the training and testing datasets with a ratio of 8:2. A generalized linear model with logit link was developed using training dataset to predict the aneurysm rupture risk based on the clinical variables and morphological features manually measured from computed tomography angiography. To facilitate the clinical application, we further constructed an easy-to-use nomogram based on the developed model.

Results Ruptured MCA aneurysm had larger aneurysm size, aneurysm height, perpendicular height, aspect ratio, size ratio, bottleneck factor, and height-width ratio. Presence of a daughter-sac was more common in ruptured than in unruptured MCA aneurysms. Six features, including aneurysm multiplicity, lobulations, size ratio, bottleneck factor, height-width ratio, and aneurysm angle, were adopted in the model after feature selection. The model achieved a relatively good performance with areas under the receiver operating characteristic curves of 0.77 in the training dataset and 0.76 in the testing dataset. The nomogram provided a visual interpretation of our model, and the rupture risk probability of MCA aneurysms can be directly read from it.

Conclusion Our model can be used to predict the rupture risk of MCA aneurysm.

Keywords Aneurysm · Computed tomography angiography · Rupture · Prediction · Morphology

Introduction

Unruptured intracranial aneurysms are detected with greater frequency with the improvement of modern imaging technique, such as digital subtraction angiography, magnetic resonance angiography, and 3-dimensional computerized tomography angiography (CTA) [1]. Aneurysm rupture is a devastating disease and is associated with a high morbidity and mortality [2, 3]. The management of these unruptured intracranial aneurysms is still controversial because of the treatment-related fatality and morbidity [4, 5]. Therefore, determining the aneurysm rupture risk is of great importance to make treatment decision for unruptured intracranial aneurysms.

In recent years, many risk factors have been found to be associated with aneurysm rupture. These risk factors include clinical characteristics, such as age, smoking, and aneurysm multiplicity [6–8], and aneurysm morphological features, such as aneurysm size, aspect ratio, and wall irregularity [9–14]. However, the relationship among the risk factors and aneurysm rupture risk is complex; accurately predicting the aneurysm rupture risk is challenging. As a powerful and promising tool, machine learning technique is capable of identifying complex relationships in large datasets [15, 16], which makes it suited to the task of aneurysm rupture risk evaluation. In recent years, machine learning has been applied to aneurysm risk prediction. A two-layer feed-forward neural network was proposed to predict the rupture risk of anterior communicating artery aneurysms and achieved a good prediction accuracy [17]. Linear and ridge regression models were developed to

✉ Yunjun Yang
yyjunjim@163.com

✉ Xiufen Jia
51376410@qq.com

[1] Department of Radiology, The First Affiliated Hospital of Wenzhou Medical University, Wenzhou, Zhejiang 325000, China

predict the stability of 420 aneurysms at different locations using morphological features extracted from PyRadiomics [18]. Most recently, support vector machine, random forest, and feed-forward artificial neural networks have been adopted for aneurysm stability assessment [19]. All the aforementioned machine learning algorithms were applied to either anterior communicating artery aneurysm or aneurysms at several locations. Aneurysm rupture risk was location dependent [20]. Few studies currently focus on the aneurysm rupture risk assessment using a large dataset of middle cerebral artery (MCA) aneurysms, although approximately 35% of all intracranial aneurysm are MCA aneurysms [21]. Moreover, these machine learning models behaved like black boxes and could not be interpretable, which might limit their application in clinics. Therefore, the purpose of this study was to evaluate the MCA aneurysm rupture risk using a machine learning method and provide a nomogram that can be practically utilized for clinical applications.

Materials and methods

Patients

This study was approved by our hospital ethics committee, and written informed consent was waived. A total of 472 patients with MCA aneurysm were found from the Electronic Medical Record System from January 2009 to October 2016. Patients were excluded if they had fusiform MCA aneurysms, or Moyamoya disease, or arteriovenous malformations. To ensure the accuracy of morphology measurement, we excluded those with poor image quality.

Image acquisition and morphology definition

We adopted three CT scanner for image acquisition, including a 320-detector row CT scanner (Aquilion ONE, Toshiba Medical Systems, Tochigi, Japan) with a section thickness of 0.5 mm and a reconstruction interval of 0.5 mm, a 64-channel multidetector CT scanner (LightSpeed VCT 64, General Electric Medical Systems, Milwaukee, WI, USA) with a section thickness of 0.625 mm and a reconstruction interval of 0.625 mm, and a 16-channel multidetector CT scanner (LightSpeed pro 16, General Electric Medical Systems, Milwaukee, WI, USA) with a section thickness of 1.25 mm and a reconstruction interval of 0.625 mm.

We reconstructed three-dimensional aneurysms from CTA images using GE Workstation ver. 4.6 and manually measured lengths and angles related to aneurysm features. Figure 1 illustrates the measurement of vessel size, aneurysm height, aneurysm width, perpendicular height, flow angle, vessel angle, parent-daughter angle, and aneurysm angle. Vessel size was determined as the average cross-sectional diameter of all arteries associated with the aneurysm. The cross-sectional diameter of a particular vessel diameter was measured by averaging the cross-sectional diameter of the artery proximal to the aneurysm neck (Via) and the cross-sectional diameter at 1.5XVia away from the aneurysm neck (Vib) (see Fig. 1), i.e., (Via+Vib)/2, i = 1, 2, or 3. Aneurysm size is the largest cross-sectional length of the aneurysm dome. Aneurysm height is the greatest distance from the center of the aneurysm neck to aneurysm dome, whereas the perpendicular height is the largest perpendicular distance from the center of aneurysm neck to the aneurysm dome. Aneurysm width is the maximal diameter perpendicular to the aneurysm height. Height-width ratio was calculated as the ratio of aneurysm width to aneurysm neck. Aspect ratio was defined as the ratio between the perpendicular height and the aneurysm neck size. Size ratio was calculated as the ratio of the aneurysm height to the vessel size. Bottleneck factor is the ratio between aneurysm width and neck size. In addition, 4 angle-related parameters were measured. Flow angle is the angle between the aneurysm height line and the vector of the blood flow in the parent artery; vessel angle is the angle between the vector of the blood flow and the aneurysm neck line; aneurysm angle represents the angle between the aneurysm neck line and the aneurysm height line; parent-daughter angle is the angle between the vector of the blood flow through the daughter vessel and the vector of the blood flow through the parent vessel.

Aneurysm lobulations include three types, i.e., regular, irregular, and daughter-sac types [17]. Locations of MCA aneurysms were divided into 4 groups: (1). aneurysms arising on the main trunk (M1) of the MCA, between the bifurcation of internal carotid artery and the main MCA bifurcation, at the origin of lenticulostriate arteries (M1-LSAAs), (2) aneurysms arising on M1 at the origin of early cortical branches (M1-ECBAs), (3) aneurysms at the main MCA bifurcation (MbifAs), and (4) aneurysms distal to the main MCA bifurcation on M2, M3, or M4 segments (MdistAs) [22]. The main projection of the MCA aneurysm [12] was determined as follows: in the axial CTA view, the aneurysm dome was grouped as anterior (in front of the MCA), posterior (behind the MCA), or neutral (neither anterior nor posterior projection); in the coronal CTA view, the aneurysm dome was categorized as superior (toward frontal lobe), inferior (toward temporal lobe), or neutral (neither superior nor inferior projection).

Model development

In this study, 80% of the included aneurysms were randomly chosen as the training dataset, and the rest were used for test. Number of features was reduced by evaluating the correlation between the features and the class, and the remaining features were further filtered by using univariate analysis. The following features were finally chosen: multiplicity, aneurysm lobulations, size ratio, bottleneck factor, height-width ratio, and

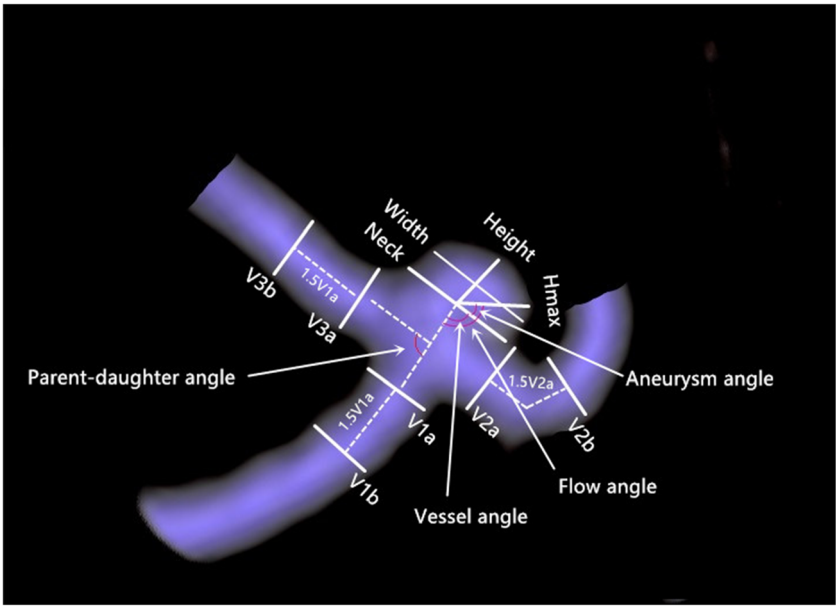

Fig. 1 Measurements of aneurysm morphological features: Via and Vib (i = 1, 2, 3), cross-section diameter of the artery; Hmax, aneurysm height

aneurysm angle. A generalized linear model with logit link (https://www.rdocumentation.org/packages/stats/versions/3.6.2/topics/glm) was developed using the selected features. The prediction accuracy of the model was quantified by the sensitivity, specificity, and the area under the receiver operating characteristic (ROC) curve (AUC). For the purpose of clinical application, we further constructed a nomogram on the basis of the developed model. A nomogram represents a graphical calculation instrument that facilitates the approximate computation of a mathematical function via intersecting lines and is designed to extract the maximum amount of information from data and provide a quick approximation of the output probability [23, 24]. R statistical software (version 3.6.1) was used for model development.

Statistical analysis

Categorical variables were presented as the frequency (percentage) and continuous variables as mean ± standard deviation. Student t-test or Mann-Whitney U tests were adopted for comparisons of continuous variables, and Fisher exact tests or χ^2 tests were applied for comparisons of categorical variables. A P value less than 0.05 was considered statistically significant. All data was analyzed using the software package SPSS 22.0 (IBM Corp, Armonk, New York).

Results

Baseline characteristics

A total of 403 patients were enrolled in this study. Of these patients, the mean age was 56.5 years old, and 231 (57.3%) were women. One hundred and thirty patients had multiple aneurysms. Table 1 shows patients' baseline information between the ruptured and unruptured MCA aneurysms. Patients with ruptured aneurysms were significantly more likely to be younger (55.1 vs. 59.5 years old), whereas patients with unruptured aneurysm were significantly more likely to have multiple aneurysms ($p < .001$). More female patients and more smoking patients had ruptured aneurysms, although the differences were not statistically significant. The main MCA bifurcation was the most common location for both ruptured and unruptured aneurysms, and patients with aneurysms at the main MCA bifurcation were more likely to be ruptured.

Morphologic characteristics between ruptured and unruptured MCA aneurysms

Table 2 demonstrates the comparison of morphological characteristics between ruptured and unruptured aneurysms. Aneurysm size, aneurysm height, and perpendicular height were significantly higher in ruptured aneurysms than in unruptured ones (P<0.05), which implied that larger aneurysms were prone to be unstable. Four ratios, including aspect ratio, size ratio, bottleneck factor, and height-width ratio, were all significantly higher in ruptured aneurysms than in unruptured ones (P<0.05). Aneurysm angle and flow angle were significantly different between the ruptured and unruptured aneurysms. Aneurysm lobulations was significantly different between the ruptured and unruptured aneurysms. Unruptured aneurysms were more frequently regular type (70.4% versus 46.4%), whereas ruptured aneurysm were more frequently daughter-sac type (29.5% versus 10.4%).

Table 1 Baseline characteristics

	All (n = 403)	Unruptured (n=125)	Ruptured (n=278)	P value
Sex (women)	231 (57.3%)	65 (52.0%)	166 (59.7%)	0.156
Age	56.5±11.7	59.5±10.7	55.1±11.9	< 0.001
Smoking (yes)	98 (24.3%)	27 (21.6%)[a]	71 (25.5%) [b]	0.515
Multiple (yes)	130 (32.3%)	66 (52.8%)	64 (23.0%)	< 0.001
Location*				<0.001
M1-LSAAs	13 (3.2%)	10 (8.0%)	3 (1.1%)	
M1-ECBAs	98 (24.3%)	35 (28.0%)	63 (22.6%)	
MbifAs	280 (69.5%)	73 (58.4%)	207 (74.5%)	
MdisAs	12 (3.0%)	7 (5.6%)	5 (1.8)	

[a] 38 missing values

[b] 25 missing values

*M1-LSAAs, aneurysms arising on the main trunk (M1) of the MCA, between the bifurcation of internal carotid artery and the main MCA bifurcation, at the origin of lenticulostriate arteries; M1-ECBAs, aneurysms arising on M1 at the origin of early cortical branches; MbifAs, aneurysms at the main MCA bifurcation; MdistAs, aneurysms distal to the main MCA bifurcation on M2, M3, or M4 segments

Nomogram for predicting rupture risk of MCA aneurysm

The generalized linear model adopted six variables, including aneurysm multiplicity, aneurysm lobulations, size ratio, bottleneck factor, height-width ratio, and aneurysm angle. Figure 2 represents the use of a nomogram to visually interpret the developed model. Application of this nomogram is simple. One can read the scoring points from the "Point" reference line according to the variable values, including aneurysm multiplicity, aneurysm lobulations, size ratio, bottleneck factor, height-width ratio, and aneurysm angle. The total points can be obtained by summing the points of each variable. According to the total points, the predicted probability of rupture risk can be read at the bottom "Probability" line.

Table 3 summarizes the prediction performance of the generalized linear model. Figure 3 illustrates the ROC curves of the developed model for both training and test datasets. The model achieved a sensitivity of 0.73 and a specificity of 0.71 in the training dataset and a sensitivity of 0.75 and a specificity of 0.72 in the test dataset. The areas under ROC curves were 0.77 (95% CI, 0.71–0.83) and 0.76 (95% CI, 0.65–0.88) for the training and testing datasets, respectively.

Discussion

In this study, we measured the morphological features of MCA aneurysm and developed a generalized linear model to predict the rupture risk of MCA aneurysm based on the measured morphological features. The model achieved a good prediction performance with AUC of 0.77 in training dataset and 0.76 in testing dataset. A nomogram was further provided to facilitate the practical application of this model in clinics.

Six features, including aneurysm multiplicity, aneurysm lobulations, size ratio, bottleneck factor, height-width ratio, and aneurysm angle, were adopted in our prediction model. Multiple aneurysms were more commonly seen in unruptured aneurysms [18], and aneurysm multiplicity was significant factor for rupture of small aneurysm [7]. Aneurysm lobulations reflect the irregularity of an aneurysm dome. Our study found that the presence of a daughter-sac was more common in ruptured aneurysms. Previous study [25] showed the strong correlation between the presence of a daughter-sac and the rupture of MCA aneurysms. The presence of a daughter aneurysm was a likely path to aneurysm rupture. A mathematical model revealed that the tensile stress in the daughter aneurysm wall first decreased to protect against rupture as the daughter aneurysm developed, and further growth of the daughter aneurysm resulted in an increase of stress and eventually led to rupture [26]. Size ratio, bottleneck factor, and height-width ratio have been reported to be related to aneurysm rupture [12]. In our study, all these three ratios were significantly higher in ruptured than in unruptured MCA aneurysms. Aneurysm angle has been shown to be a promising morphological metric for intracranial aneurysm rupture risk assessment [27].

Great efforts have been exerted for evaluating the aneurysm rupture risk. Morphological analysis, hemodynamic analysis, and clinical factor assessment have been performed to find the risk factors of aneurysm rupture [27–29]. A few approaches, such as scoring system and machine learning models, have been proposed to predict the aneurysm rupture risk using these risk factors. A PHASES score system [6] has been developed from a prospective cohort study. This score

Table 2 Morphological characteristics between ruptured and unruptured MCA aneurysm

	All (*n*=403)	Unruptured (*n*=125)	Ruptured (*n*=278)	*P* value
Aneurysm size (mm)	6.49±3.27	5.76±3.33	6.82±3.20	0.002
Vessel size (mm)	2.30±0.58	2.40±0.63	2.27±0.55	0.036
Aneurysm height (mm)	4.99±2.83	4.17±2.99	5.35±2.68	<0.001
Perpendicular height (mm)	4.10±2.49	3.59±2.78	4.33±2.32	0.006
Width (mm)	4.71±2.55	4.41±2.59	4.85±2.52	0.112
Neck size (mm)	3.92±1.62	4.00±1.63	3.88±1.61	0.499
Aspect ratio	1.09±0.58	0.92±0.59	1.17±0.56	<0.001
Size ratio	2.34±1.58	1.80±1.30	2.58±1.63	<0.001
Bottleneck factor	1.24±0.56	1.12±0.52	1.30±0.57	0.004
Height-width ratio	0.87±0.23	0.79±0.20	0.91±0.24	<0.001
Aneurysm angle	64.2±19.0	67.9±18.4	62.6±10.1	0.01
Vessel angle	62.1±32.1	55.7±28.7	64.9±33.2	0.008
Flow angle	134.3±29.1	132.7±29.6	135.1±29.0	0.462
Parent-daughter angle	79.3±23.3	80.4±24.2	78.8±23.0	0.525
Aneurysm lobulations				<0.001
Regular type	217 (53.8%)	88 (70.4%)	129 (46.4%)	
Irregular type	91 (22.6%)	24 (19.2%)	67 (24.1%)	
Daughter-sac type	95 (23.6%)	13 (10.4%)	82 (29.5%)	
Projection in axial CTA				0.117
Anterior	221 (54.8%)	59 (47.2%)	162 (58.3%)	
Posterior	73 (18.1%)	27 (21.6%)	46 (16.5%)	
Neutral	109 (27%)	39 (31.2%)	70 (25.2%)	
Projection in coronal CTA				0.990
Superior	118 (29.3%)	36 (28.8%)	82 (29.5%)	
Inferior	128 (31.8%)	40 (32.0%)	88 (31.7%)	
Neutral	157 (39.0%)	49 (39.2%)	108 (38.8%)	
Hypoplastic A1				0.996
No	315 (78.2%)	98 (78.4%)	217 (78.1%)	
Ipsilateral	46 (11.4%)	14 (11.2%)	32 (11.5%)	
Contralateral	42 (10.4%)	13 (10.4%)	29 (10.4%)	
Hypoplastic PCoA				0.864
No	69 (17.1%)	21 (16.8%)	48 (17.3%)	
Ipsilateral	56 (13.9%)	15 (12.0%)	41 (14.7%)	
Contralateral	63 (15.6%)	19 (15.2%)	44 (15.8%)	
Both	215 (53.3%)	70 (56.0%)	145 (52.2%)	
Fetal PCoA				0.974
No	292 (72.5%)	91 (72.8%)	201 (72.3%)	
Ipsilateral	39 (9.7%)	13 (10.4%)	26 (9.4%)	
Contralateral	45 (11.2%)	13 (10.4%)	32 (11.5%)	
Both	27 (6.7%)	8 (6.4%)	19 (6.8%)	

MCA middle cerebral artery, *CTA* computed tomography angiography, *PCoA* posterior communicating artery

system used age, hypertension, a history of subarachnoid hemorrhage, aneurysm size, aneurysm location, and geographical region as predictors and was found to be an easily applicable aid for the aneurysm rupture analysis. Recent studies [30, 31], however, demonstrated that the PHASES score might only provide a weak tool for evaluating aneurysm rupture risk, and parameters beyond the features of the PHASES score might be needed to improve the prediction accuracy. With the advance of artificial intelligence, machine learning technique has been applied for aneurysm rupture risk prediction. A feed-forward artificial neural network was successfully used to predict the rupture risk of anterior

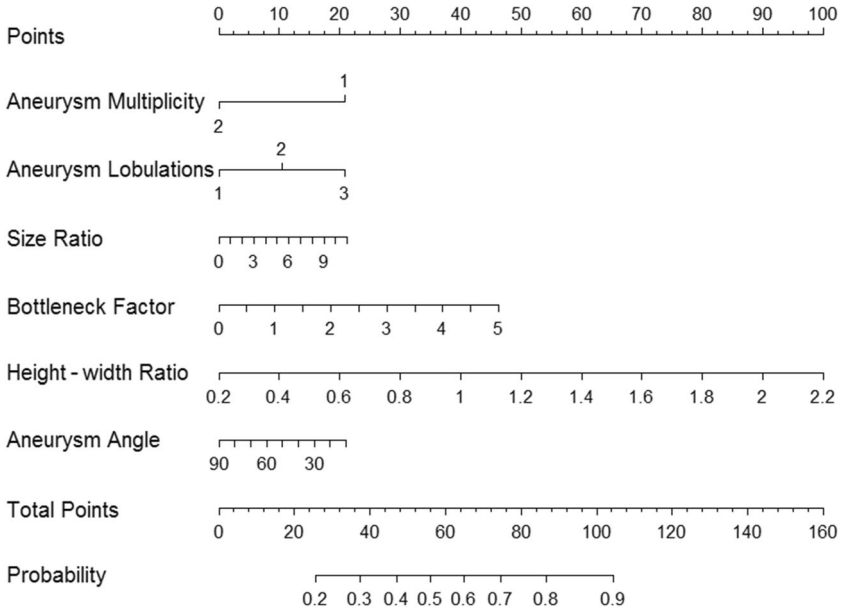

Fig. 2 Nomogram to predict the rupture risk of MCA aneurysms. Aneurysm multiplicity: 1 (single aneurysm) and 2 (multiple aneurysms). Aneurysm lobulations: 1 (regular type), 2 (irregular type), and 3 (daughter-sac type)

communicating artery aneurysms based on patients' basic characteristics and aneurysm morphological features [17]. Random forest, linear support vector machine, and radial basis function kernel support vector machine models were applied to classify aneurysm rupture status at different locations, and it was found that aneurysm location and size were the strongest predictors of aneurysm rupture and machine learning models were robust tools in predicting aneurysm rupture risk [32]. Linear, ridge, and lasso regression models were developed to predict the stability of 420 aneurysms at different locations based on PyRadiomics-derived morphological features; it was found that the extracted features were useful for aneurysm stratification and the developed models could be used for the prediction of aneurysm stability [18]. Recently, a random forest machine learning algorithm was applied to classify the rupture status of 226 intracranial aneurysms at different locations using only morphologic variables (model 1), only hemodynamic parameters (model 2), and both morphologic and hemodynamic parameters (model 3); corresponding accuracy was 77.0% for model 1, 71.2% for model 2, and 78.3% for model 3 [33]. These machine learning methods mentioned above were applied in either anterior communicating artery aneurysm or aneurysms at different locations. To date, application of machine learning technique to predict the rupture risk of MCA aneurysm has been rarely reported. In this study, we enrolled 403 MCA aneurysms. A generalized linear model was constructed to predict the rupture risk of MCA aneurysm, and a relatively good prediction performance was achieved. More important, a nomogram, as a model visualization figure, provided a simple and easy tool for the practical application of the developed model in clinics.

Limitations

There were several limitations in this study. First, this was retrospective and single-center study, and only Chinese population were involved. Previous research has shown that aneurysm rupture risk is population dependent [6]. Generalization of our model to other population may not be satisfied. Second, aneurysm growth is a dynamic process, and aneurysm may evolve before rupture. However, we did not perform long-term follow-up study to monitor unruptured aneurysm over time because of the ethical dilemma and patients' safety issue [34]. Third, we did not test our model using external dataset. Further external validation in a large independent population is still required. Finally, our model includes only radiological data regarding the aneurysms, and no clinical data are included, which may limit the application of our model. Many clinical factors have been reported to be associated with intracranial aneurysm rupture [35, 36]; however,

Table 3 Prediction accuracy of the developed model

Dataset	Sensitivity	Specificity	AUC (95% confidence interval)
Training dataset	0.73	0.71	0.77 (0.71–0.83)
Testing dataset	0.75	0.72	0.76 (0.65–0.88)

AUC area under the receiver operating characteristic curve

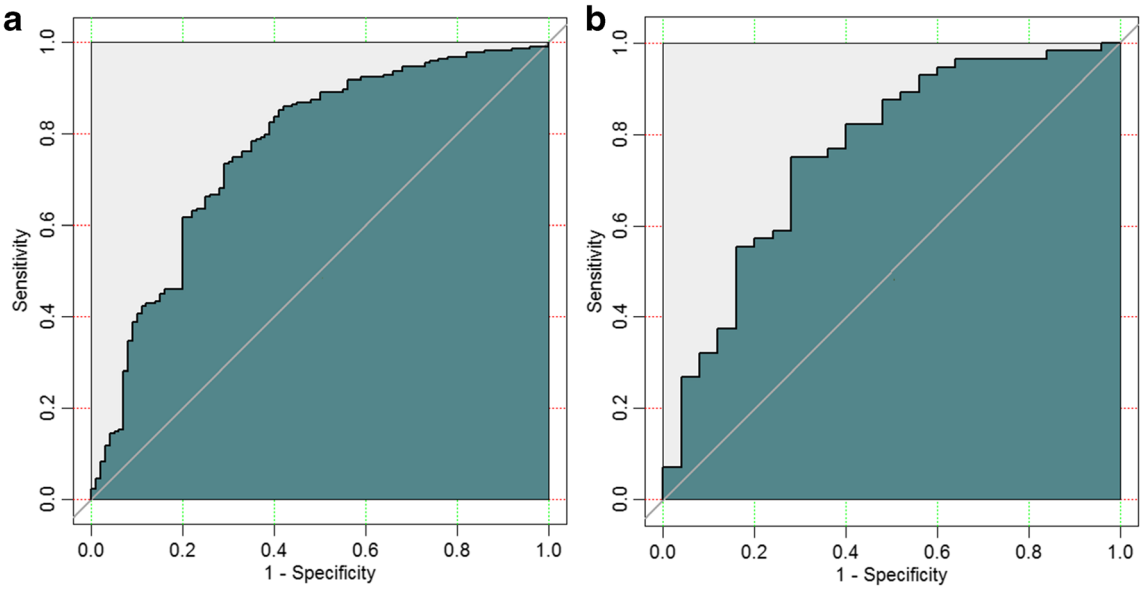

Fig. 3 Receiver operating characteristic (ROC) curves developed for (**a**) training dataset and (**b**) testing dataset

only several clinical parameters were considered in this study due to the retrospective design. Future work considering more clinical data is still needed. Nevertheless, our work may be considered as a starting point for the development of further clinical-radiological models that may guide physicians to make treatment decision for each single patient.

Conclusions

In summary, we examined the risk factors from a large MCA aneurysm dataset and developed a classification machine learning model to predict rupture status of MCA aneurysms. In addition, we constructed an easy to use nomogram tool for the practical application purpose, which might facilitate the treatment optimization.

Author contribution Jinjin Liu, Xiufen Jia, and Yunjun Yang contributed to the study conception and design. Material preparation, data collection, and analysis were performed by Jinjin Liu, Xiufen Jia, Jiafeng Zhou, Boli Lin, Dongqing Zhu, Qiong Li, and Zhonggang Chen. The first draft of the manuscript was written by Jinjin Liu, and all authors commented on previous versions of the manuscript. All authors read and approved the final manuscript.

Funding This study was supported by the Basic Research Project of Wenzhou (Y2020166), Wenzhou Major Program of Science and Technology Innovation (ZY2020012), Health Foundation for Creative Talents in Zhejiang Province, China (No.2016), and Natural Science Foundation of Zhejiang Province, China (Grant No. LQ15H180002).

Data Availability The datasets analyzed during the current study are available from the corresponding author on a reasonable request.

Declarations

Conflict of interest The authors declare no competing interests.

Ethical approval This study was approved by the ethical committee of the First Affiliated Hospital of Wenzhou Medical University.

Informed consent Informed consent was obtained from all patients involved in the study.

References

1. Rustemi O, Alaraj A, Shakur SF, Orning JL, Du X, Aletich VA, Amin-Hanjani S, Charbel FT (2015) Detection of unruptured intracranial aneurysms on noninvasive imaging. Is there still a role for digital subtraction angiography? Surg Neurol Int 6:175
2. van Gijn J, Kerr RS, Rinkel GJE (2007) Subarachnoid haemorrhage. Lancet 369(9558):306–318
3. Yu Z, Zheng J, Guo R, Li M, Li H, Ma L, You C (2020) The accuracy of aneurysm size in predicting rebleeding after subarachnoid hemorrhage: a meta-analysis. Neurol Sci 41(7):1843–1850
4. Thompson BG, Brown R Jr, Amin-Hanjani S, Broderick JP, Cockroft KM, Connolly E Jr, Duckwiler GR, Harris CC, Howard VJ, Johnston SC (2015) Guidelines for the management of patients with unruptured intracranial aneurysms: a guideline for healthcare professionals from the American Heart Association/American Stroke Association. Stroke 46(8):2368–2400
5. Etminan N, Rinkel GJ (2016) Unruptured intracranial aneurysms: development, rupture and preventive management. Nat Rev Neurol 12:699–713
6. Greving JP, Wermer MJ, Brown RD, Morita A, Juvela S, Yonekura M, Ishibashi T, Torner JC, Nakayama T, Rinkel GJ (2014) Development of the PHASES score for prediction of risk of rupture of intracranial aneurysms: a pooled analysis of six prospective cohort studies. Lancet Neurol 13(1):59–66

7. Sonobe M, Yamazaki T, Yonekura M, Kikuchi H (2010) Small unruptured intracranial aneurysm verification study. Stroke 41(9): 1969–1977
8. Xia N, Liu Y, Zhong M, Zhuge Q, Fan L, Chen W, Yang Y, Zhao B (2016) Smoking associated with increased aneurysm size in patients with anterior communicating artery aneurysms. World Neurosurg 87:155–161
9. Kirino T, Hashi K, Neuro P (2012) The natural course of unruptured cerebral aneurysms in a Japanese cohort. N Engl J Med 366(26):2474
10. Ujiie H, Tamano Y, Sasaki K, Hori T (2001) Is the aspect ratio a reliable index for predicting the rupture of a saccular aneurysm? Neurosurgery 48(3):495–503
11. Wiebers DO (2003) Unruptured intracranial aneurysms: natural history, clinical outcome, and risks of surgical and endovascular treatment. Lancet 362(9378):103–110
12. Elsharkawy A, Lehecka M, Niemela M, Kivelev J, Billongrand R, Lehto H, Kivisaari R, Hernesniemi J (2013) Anatomic risk factors for middle cerebral artery aneurysm rupture: computed tomography angiography study of 1009 consecutive patients. Neurosurgery 73(5):825–837
13. Jiang P, Liu Q, Wu J, Chen X, Li M, Li Z, Yang S, Guo R, Gao B, Cao Y, Wang S (2018) A novel scoring system for rupture risk stratification of intracranial aneurysms: a hemodynamic and morphological study. Front Neurosci 12:596
14. Xu Z, Kim BS, Lee KS, Choi JH, Shin YS (2019) Morphological and clinical risk factors for the rupture of posterior communicating artery aneurysms: significance of fetal-type posterior cerebral artery. Neurol Sci 40(11):2377–2382
15. Tafti AP, Larose E, Badger JC, Kleiman R, Peissig PL (2017) Machine learning-as-a-service and its application to medical informatics. In: machine learning and data mining in pattern recognition. p 206-219
16. Ker J, Wang L, Rao J, Lim T (2018) Deep learning applications in medical image analysis. IEEE Access 6:9375–9389
17. Liu J, Chen Y, Lan L, Lin B, Chen W, Wang M, Li R, Yang Y, Zhao B, Hu Z, Duan Y (2018) Prediction of rupture risk in anterior communicating artery aneurysms with a feed-forward artificial neural network. Eur Radiol 28(8):3268–3275
18. Liu Q, Jiang P, Jiang Y, Ge H, Li S, Jin H, Li Y (2019) Prediction of aneurysm stability using a machine learning model based on pyradiomics-derived morphological features. Stroke 50(9):2314–2321
19. Zhu W, Li W, Tian Z, Zhang Y, Yang X (2020) Stability assessment of intracranial aneurysms using machine learning based on clinical and morphological features. Transl Stroke Res (7)
20. Forget TR Jr, Benitez R, Veznedaroglu E, Sharan A, Mitchell W, Silva M, Rosenwasser RH (2001) A review of size and location of ruptured intracranial aneurysms. Neurosurgery 49(6):1322–1326
21. Vlak MHM, Algra A, Brandenburg R, Rinkel GJE (2011) Prevalence of unruptured intracranial aneurysms, with emphasis on sex, age, comorbidity, country, and time period: a systematic review and meta-analysis. Lancet Neurol 10(7):626–636
22. Elsharkawy A, Lehecka M, Niemela M, Billongrand R, Lehto H, Kivisaari R, Hernesniemi J (2013) A new, more accurate classification of middle cerebral artery aneurysms: computed tomography angiographic study of 1,009 consecutive cases with 1,309 middle cerebral artery aneurysms. Neurosurgery 73(1):94–102
23. Shariat SF, Karakiewicz PI, Godoy G, Lerner SP (2009) Use of nomograms for predictions of outcome in patients with advanced bladder cancer. Ther Adv Urol 1(1):13–26
24. Ing E, Ing R (2018) The use of a nomogram to visually interpret a logistic regression prediction model for giant cell arteritis. Neuro-Ophthalmology 42(5):284–286
25. Zhang J, Can A, Mukundan S, Steigner ML, Castro VM, Dligach D, Finan S, Yu S, Gainer VS, Shadick NA (2019) Morphological variables associated with ruptured middle cerebral artery aneurysms. Neurosurgery 85(1):75–83
26. Meng H, Feng Y, Woodward SH, Bendok BR, Hanel RA, Guterman LR, Hopkins LN (2005) Mathematical model of the rupture mechanism of intracranial saccular aneurysms through daughter aneurysm formation and growth. Neurol Res 27(5):459–465
27. Dhar S, Tremmel M, Mocco J, Kim M, Yamamoto J, Siddiqui AH, Hopkins LN, Meng H (2008) Morphology parameters for intracranial aneurysm rupture risk assessment. Neurosurgery 63(2):185–197
28. Xiang J, Tutino VM, Snyder KV, Meng H (2014) CFD: computational fluid dynamics or confounding factor dissemination? The role of hemodynamics in intracranial aneurysm rupture risk assessment. AJNR Am J Neuroradiol 35(10):1849–1857
29. Murayama Y, Takao H, Ishibashi T, Saguchi T, Ebara M, Yuki I, Arakawa H, Irie K, Urashima M, Molyneux AJ (2016) Risk analysis of unruptured intracranial aneurysms: prospective 10-year cohort study. Stroke 47(2):365–371
30. Neyazi B, Sandalcioglu IE, Maslehaty H (2019) Evaluation of the risk of rupture of intracranial aneurysms in patients with aneurysmal subarachnoid hemorrhage according to the PHASES score. Neurosurg Rev 42(2):489–492
31. Pagiola I, Mihalea C, Caroff J, Ikka L, Chalumeau V, Iacobucci M, Ozanne A, Gallas S, Marques M, Nalli D, Carrete H, Caldas JG, Frudit ME, Moret J, Spelle L (2019) The PHASES score: to treat or not to treat? Retrospective evaluation of the risk of rupture of intracranial aneurysms in patients with aneurysmal subarachnoid hemorrhage. J Neuroradiol 47:349–352
32. Silva MA, Patel J, Kavouridis VK, Gallerani T, Beers A, Chang K, Hoebel K, Brown JA, See AP, Gormley WB (2019) Machine Learning models can detect aneurysm rupture and identify clinical features associated with rupture. World Neurosurg 131:e46–e51
33. Tanioka S, Ishida F, Yamamoto A, Shimizu S, Sakaida H, Toyoda M, Kashiwagi N, Suzuki H (2020) Machine learning classification of cerebral aneurysm rupture status with morphologic variables and hemodynamic parameters. Radiology: Artific Intell 2(1):e190077
34. Lall RR, Eddleman CS, Bendok BR, Batjer HH (2009) Unruptured intracranial aneurysms and the assessment of rupture risk based on anatomical and morphological factors: sifting through the sands of data. Neurosurg Focus 26(5):E2
35. Kleinloog R, de Mul N, Verweij BH, Post JA, Rinkel GJE, Ruigrok YM (2017) Risk Factors for intracranial aneurysm rupture: a systematic review. Neurosurgery 82(4):431–440
36. Signorelli F, Sela S, Gesualdo L, Chevrel S, Tollet F, Pailler-Mattei C, Tacconi L, Turjman F, Vacca A, Schul DB (2018) Hemodynamic stress, inflammation, and intracranial aneurysm development and rupture: a systematic review. World Neurosurg 115: 234–244